

Article

## Photocatalytic Degradation of Methyl Orange over Metalloporphyrins Supported on TiO<sub>2</sub> Degussa P25

Xian-Tai Zhou, Hong-Bing Ji \* and Xing-Jiao Huang

School of Chemistry and Chemical Engineering, Key Laboratory of Low-Carbon Chemistry & Energy Conservation of Guangdong Province, Sun Yat-sen University, 510275, Guangzhou, China

\* Author to whom correspondence should be addressed; E-Mail: jihb@mail.sysu.edu.cn;  
Tel.: +86-20-841-13658; Fax: +86-20-841-13654.

Received: 21 November 2011; in revised form: 11 January 2012 / Accepted: 16 January 2012 /  
Published: 25 January 2012

---

**Abstract:** The photocatalytic activity of *meso*-tetraphenylporphyrins with different metal centers (Fe, Co, Mn and Cu) adsorbed on TiO<sub>2</sub> (Degussa P25) surface has been investigated by carrying out the photodegradation of methyl orange (MO) under visible and ultraviolet light irradiation. The photocatalysts were characterized by X-ray diffraction (XRD), scanning electron microscopy (SEM), diffuse reflectance UV (DRS-UV-vis) and infrared spectra. Copper porphyrin-sensitized TiO<sub>2</sub> photocatalyst (CuP-TiO<sub>2</sub>) showed excellent activity for the photodegradation of MO whether under visible or ultraviolet light irradiation. Natural Bond Orbital (NBO) charges analysis showed that methyl orange ion is adsorbed easier by CuP-TiO<sub>2</sub> catalyst due to the increase of induced interactions.

**Keywords:** metalloporphyrins; photocatalytic; methyl orange; degradation

---

### 1. Introduction

Due to its nontoxicity, stability, high photocatalytic activity and recyclability the photocatalytic degradation of pollutants on the surface of titanium dioxide (TiO<sub>2</sub>) has been intensively studied as a way to solve environmental problems [1–3]. Despite the many known advantages of using TiO<sub>2</sub>, it suffers from the shortcoming of having a large band gap (~3.2 eV) which restricts its use to the ultraviolet region. Such radiation is not very abundant in the solar radiation that reaches the Earth, which limits the use of TiO<sub>2</sub> in solar energy utilization [4]. Therefore, many methods have been

applied to extend the light absorption of TiO<sub>2</sub> [5–10], in which photosensitization has shown excellent capability compared with other methods such as metals ion doping.

In the past decades, metalloporphyrins have been used as cytochrome P-450 models for the highly efficient homogeneous or heterogeneous oxidation of organic compounds [11–16]. Moreover, they are recognized to be the most promising photosensitizers due to their very strong absorption in the 400–500 nm region (Soret band) and in the 500–700 nm region (Q bands) [17]. Recent years, porphyrins-sensitized TiO<sub>2</sub> photocatalyst have been used for the degradation of pollutants. Li and co-authors reported the efficient degradation of 4-nitrophenol (4-NP) under visible light irradiation, in which the complex structural porphyrins was used as photosensitizer [18]. Tetra(4-carboxyphenyl) metalloporphyrins adsorbed on TiO<sub>2</sub> surface were used as sensitizers for the degradation of atrazine under visible light irradiation [19].

However, in the treatments of methyl orange (MO) azo dye waste, little attention has been paid on the photocatalytic degradation with porphyrins-sensitized TiO<sub>2</sub> composites as catalyst [20]. In the present work, the photocatalytic degradation of methyl orange catalyzed by the simple structural metalloporphyrins (*meso*-tetraphenylmetalloporphyrins) immobilized on TiO<sub>2</sub> (Degussa P25) has been investigated. Moreover, NBO charges analysis was performed with density functional theory (DFT) in order to explore the influence of metal ion on the photocatalytic activity.

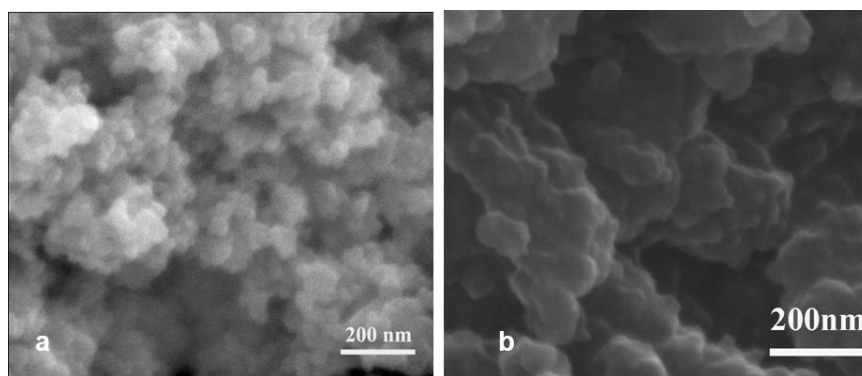
## 2. Results and Discussion

### 2.1. Characterization of the Photocatalysts

#### 2.1.1. SEM Images

The morphology of the photocatalysts was examined by scanning electron microscope (SEM). The micrographs of pure TiO<sub>2</sub> and CuP-TiO<sub>2</sub> are shown in Figures 1(a) and (b), respectively. Figure 1(a) shows the typical surface of TiO<sub>2</sub> Degussa P25, with the average crystallite size about 20 nm. When metalloporphyrins was doped on the TiO<sub>2</sub>, aggregates could be observed clearly from the micrographs of CuP-TiO<sub>2</sub> as shown in Figure 1(b), which indicated the strong adsorption occurred between metalloporphyrins and the TiO<sub>2</sub> support.

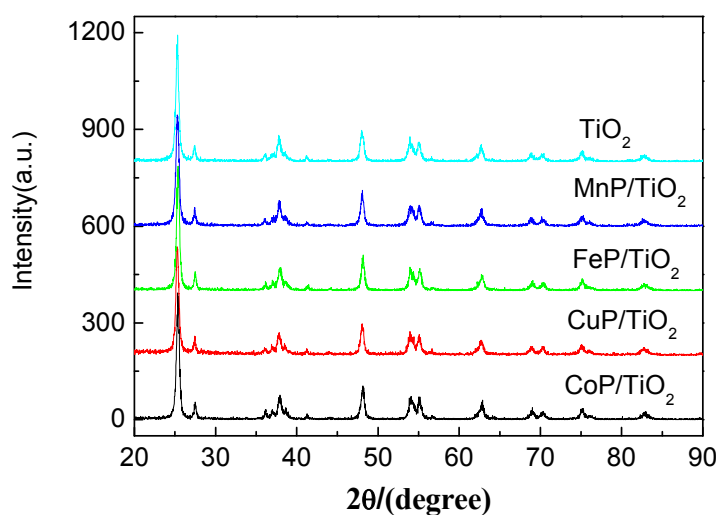
**Figure 1.** SEM image of TiO<sub>2</sub> (a) and CuP-TiO<sub>2</sub> (b).



### 2.1.2. XRD Analysis

The crystal phases of TiO<sub>2</sub> and different metalloporphyrins-TiO<sub>2</sub> catalysts were analyzed by means of X-ray diffraction, as shown in Figure 2. For TiO<sub>2</sub> Degussa P25, the peaks at 25.3° and 27.4° are the characteristic reflection for anatase and rutile, respectively [21]. It could be known that the structure of metalloporphyrins-immobilized TiO<sub>2</sub> are unchanged to those observed for the bare TiO<sub>2</sub>, indicating that the immobilization process did not destroy the characteristic structure of TiO<sub>2</sub>.

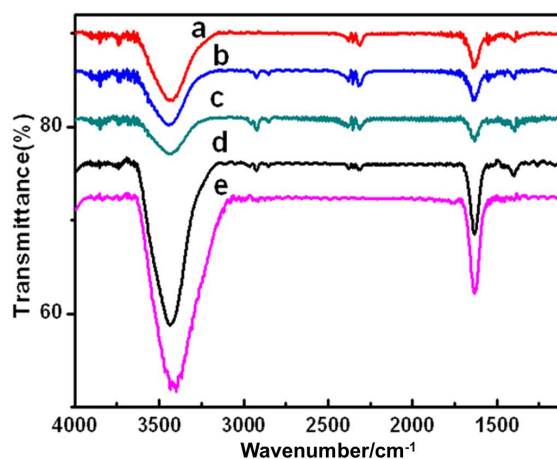
**Figure 2.** X-ray diffraction patterns of TiO<sub>2</sub> (P25) and metalloporphyrins-TiO<sub>2</sub> catalysts.



### 2.1.3. FT-IR spectra

The bonding characteristics of functional groups in TiO<sub>2</sub> and different metalloporphyrins-TiO<sub>2</sub> composites were identified by FT-IR spectroscopy as shown in Figure 3. A broad band at 3425 cm<sup>-1</sup> is the primary O-H stretching of the hydroxyl functional group. The band around 1630 cm<sup>-1</sup> is attributed to the bending vibration H-OH groups for TiO<sub>2</sub> Degussa P25.

**Figure 3.** FTIR spectra of TiO<sub>2</sub> (P25) and metalloporphyrins-TiO<sub>2</sub> catalysts, (a): CoP-TiO<sub>2</sub>, (b): FeP-TiO<sub>2</sub>, (c): MnP-TiO<sub>2</sub>, (d): CuP-TiO<sub>2</sub>, (e): TiO<sub>2</sub> (P25).



After metalloporphyrins was immobilized on TiO<sub>2</sub>, the basic characteristic peaks for TiO<sub>2</sub> hardly changed. The stretching vibrations of C-C, C-H bonds can be observed in the supported catalysts, indicating that there contains metalloporphyrins on the surface of TiO<sub>2</sub>. These changes indicated the presence of metalloporphyrins was immobilized onto TiO<sub>2</sub> Degussa P25. Further observation shows that the peaks corresponding to the stretching vibrations of hydroxyl groups are broader and stronger in TiO<sub>2</sub> than that of supported catalysts, indicating that the decrease of hydroxyl groups after metalloporphyrins is immobilized onto TiO<sub>2</sub>.

#### 2.1.4. DR UV-vis Spectra

The presence of metalloporphyrins in the TiO<sub>2</sub> Degussa P25 was determined by UV-Vis diffuse reflectance (UV-Vis-DRS) as shown in Figure 4. The UV-Vis spectra of metalloporphyrins using CH<sub>2</sub>Cl<sub>2</sub> as a solvent were recorded on a Shimadzu UV-2450 UV-Vis spectrophotometer in the range of 200–800 nm, and all results were summarized in Table 1.

**Figure 4.** The diffuse reflectance spectra of TiO<sub>2</sub> (P25) and metalloporphyrins-TiO<sub>2</sub> catalysts, (a): TiO<sub>2</sub> (P25), (b): CuP-TiO<sub>2</sub>, (c): CoP-TiO<sub>2</sub>, (d): MnP-TiO<sub>2</sub>, (e): FeP-TiO<sub>2</sub>.

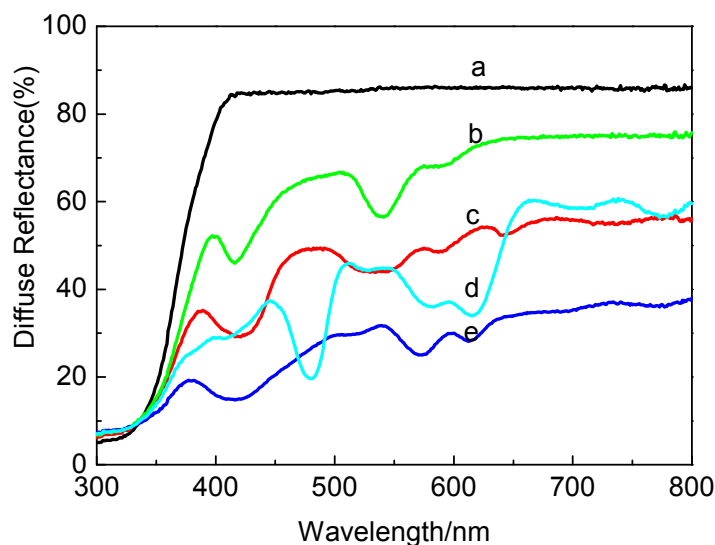


**Table 1.** UV-vis data of metalloporphyrins and DR data of photocatalysts.

Compounds	$\lambda_{\max}$ (nm)			
FeP	416	513	569	603
FeP-TiO <sub>2</sub>	413	517	587	612
CoP	410	527	580	635
CoP-TiO <sub>2</sub>	412	530	589	642
MnP	407	477	574	609
MnP-TiO <sub>2</sub>	410	479	577	615
CuP	414	538	586	619
CuP-TiO <sub>2</sub>	418	540	590	622

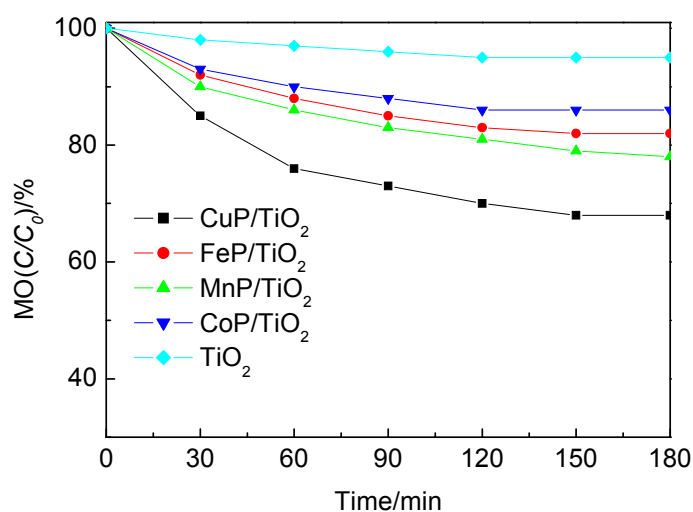
Obviously, there is no absorption above 400 nm for TiO<sub>2</sub>, while the supported catalysts exhibit the characteristic peaks of metalloporphyrins (Table 1), indicating that metalloporphyrins successfully

loaded onto the  $\text{TiO}_2$  surface while maintaining the porphyrin framework. It was further observed that the DR spectra of the photocatalysts had a significant red shift compared with the metalloporphyrins in  $\text{CH}_2\text{Cl}_2$  solution, respectively. The red shift could be interpreted as the result of an absorption between the metalloporphyrins and  $\text{TiO}_2$  surface.

## 2.2. Photocatalytic Activity

Firstly, the photocatalytic activities of  $\text{TiO}_2$  (P25) and the supported catalysts were measured by the degradation of methyl orange aqueous solution under visible light irradiation. The residual concentration ratios  $c/c_0$  of MO versus degradation time ( $t$ ) was shown in Figure 5.

**Figure 5.** Photodegradation of MO by  $\text{TiO}_2$  and MP- $\text{TiO}_2$  catalysts under visible light irradiation.

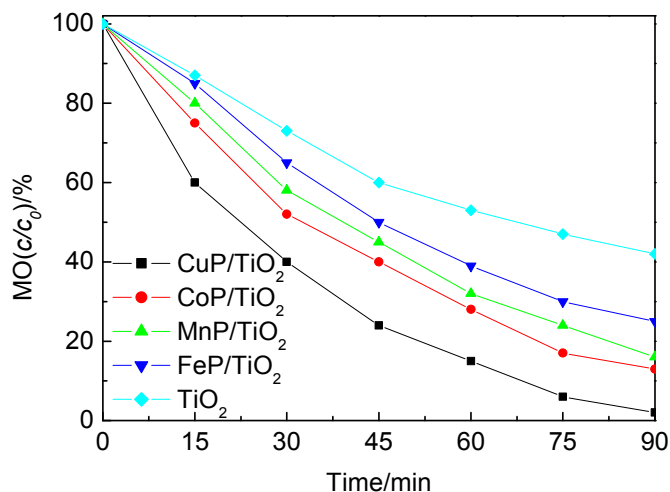


In Figure 5,  $c_0$  is the initial concentration of MO, and  $c$  is the concentration of MO after visible light irradiation. As shown in Figure 5,  $\text{TiO}_2$  presented poor activity for the degradation of MO under visible light irradiation, which the degradation ratio was less than 10% even the irradiation time reached up to 180 min. It could be seen that all MP- $\text{TiO}_2$  ( $M = \text{Fe}, \text{Co}, \text{Mn}$  and  $\text{Cu}$ ) showed higher photocatalytic activity than the bare  $\text{TiO}_2$  Degussa P25. Among these MP- $\text{TiO}_2$  catalysts,  $\text{CuP-TiO}_2$  exhibited the best efficiency for the degradation of MO. The efficiency of the supported catalysts was found to follow the order:  $\text{CuP-TiO}_2 > \text{MnP-TiO}_2 > \text{FeP-TiO}_2 > \text{CoP-TiO}_2$ .

When the degradation reaction of MO was conducted under ultraviolet light irradiation, the photocatalytic efficiencies of all samples were extremely enhanced compared with those observed under visible light conditions and the results were shown in Figure 6. The results indicate that the activities of MP- $\text{TiO}_2$  are higher than those of  $\text{TiO}_2$ . Compared with other supported catalysts,  $\text{CuP-TiO}_2$  also exhibited the best efficiency for the degradation of MO under UV light irradiation, which the degradation ratio reached up to 98% after 1.5 h of irradiation. The efficiency of the catalysts was found to follow the order:  $\text{CuP-TiO}_2 > \text{CoP-TiO}_2 > \text{MnP-TiO}_2 > \text{FeP-TiO}_2$ . These results indicate that metal ion plays an important role in the photoreactivity. With the partially filled  $d$  orbitals,  $\text{Cu(II)}$  ions are capable of fluorescence quenching by electron or energy transfer [22]. In addition, according to the diffuse reflectance spectra as listed in Table 1,  $\text{CuP-TiO}_2$  has more adsorption compared with

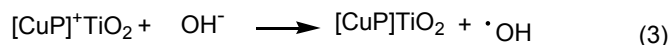
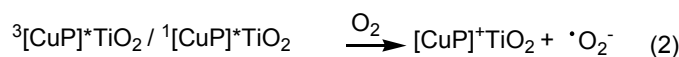
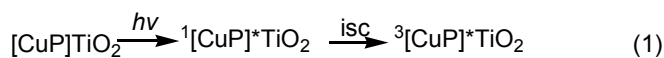
other metalloporphyrins supported on TiO<sub>2</sub> composite catalysts, especially in the longer wavelength, which is also responsible for the high efficiency of Cu-TiO<sub>2</sub>.

**Figure 6.** Photodegradation of MO by TiO<sub>2</sub> and MP-TiO<sub>2</sub> catalysts under ultraviolet light irradiation.



As discussed above, TiO<sub>2</sub> Degussa P25 impregnated with metalloporphyrins were more efficient catalysts compared to bare TiO<sub>2</sub> for the photodegradation of MO no matter whether under visible or ultraviolet light irradiation. Metalloporphyrins attached to TiO<sub>2</sub> could facilitate the charge transfer between the TiO<sub>2</sub> valence band and the methyl orange molecules. The metal ions may adsorb the MO molecules and encourage the charge-transfer process.

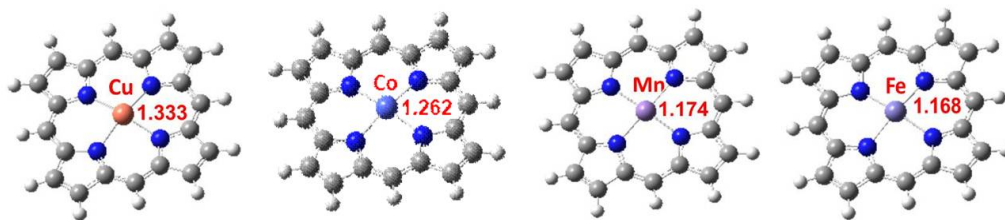
According to previous report [23–26], the process of CuP-TiO<sub>2</sub> photocatalytic reaction can be initiated by the excitation of the ground state of the sensitizer (CuP) *via* one photon transition ( $h\nu$ ) to its singlet excited state <sup>1</sup>[CuP]\*. Triplet state <sup>3</sup>[CuP]\* of the sensitizer could be generated by a process of intersystem crossing (equation 1). Both excited states can produce  $\cdot\text{O}_2^-$  with molecular oxygen under irradiation (equation 2). Following a series of reactions produce reactive intermediate such as  $\cdot\text{OH}$  could also be generated (equation 3).



To get a better understanding for the influence of metal ion on the photocatalytic activity, calculations were performed with the Gaussian03W package using the density functional theory (DFT) [27]. Full geometry optimizations of different metalloporphyrins were performed employing Becke's three parameter Lee-Yang-Parr correlation functions (B3LYP) combined with 6-31G basis set. The optimized structures of MP-TiO<sub>2</sub> (M= Fe, Co, Mn and Cu) are presented in Figure 7.

According to the calculated results, the NBO charge of metal ion for CuP, CoP, FeP and MnP are 1.333, 1.262, 1.174 and 1.168 eV, respectively. It is well known that methyl orange is an anionic dye. Therefore, the interaction between positively charged surface of the supported catalysts and MO ion could happen.

**Figure 7.** The optimized molecular structures of the metalloporphyrins with different metal ion.



Due to the higher positive NBO charge of CuP, the methyl orange ion is easily adsorbed by CuP-TiO<sub>2</sub> catalyst due to the increase of induced interaction, resulting in higher photocatalytic activity. In addition, for the metalloporphyrins with different metal ions, the order of activity under ultraviolet light irradiation is exactly consistent with the calculated NBO charge orders of the metal ions, which indicates the interaction between MO and catalyst is the key step for the photocatalytic degradation.

### 3. Experimental

#### 3.1. Preparation of the Metalloporphyrins

All chemical reagents were of analytical grade and were used without further purification unless indicated. Pyrrole was redistilled before use. Metalloporphyrins catalysts were prepared according to the previous procedures [28]. The structures of catalysts were confirmed by elementary analysis, IR and UV-Vis spectra. FT-IR spectra were obtained on a Bruker 550 spectrometer. UV-Vis spectra were recorded on a Shimadzu UV-2450 UV-Vis spectrophotometer. Elemental analysis data were obtained on Vario EL III.

#### 3.2. Preparation of the Photocatalysts

In this work, TiO<sub>2</sub> Degussa P25 (75% anatase and 25% rutile form, surface area  $50 \pm 15$  m<sup>2</sup>/g) was used for the immobilization of the simple structural metalloporphyrins (Fe, Co, Mn and Cu). The loaded samples used as photocatalyst for the degradation experiments were prepared in the following way: metalloporphyrins (12  $\mu$ mol) was dissolved in CH<sub>2</sub>Cl<sub>2</sub> (30 mL) and TiO<sub>2</sub> (P25, 2 g) was added to this solution. The resulting suspension was magnetically stirred at room temperature for 10 h. The catalyst was collected by removing solvent under vacuum and dried at 60 °C for 12 h. The photocatalyst was marked as FeP-TiO<sub>2</sub>, CoP-TiO<sub>2</sub>, MnP-TiO<sub>2</sub> and CuP-TiO<sub>2</sub>, respectively.

The surface morphology and composition of the samples were investigated by scanning electron microscopy (Quanta 400F) with energy dispersive X-ray (EDX) spectroscopy. The crystalline structure of the samples was determined by an X-ray diffraction (XRD) using a Rigaku D/MAX-RB diffractometer with Cu K $\alpha$  source and operated at 40 kV and 40 mA. The diffraction patterns were recorded in the  $2\theta$  value range of 20–90° with a scanning rate of 10 °/min. UV-Vis spectra were recorded on a Shimadzu UV-2450 UV-Vis spectrophotometer. FT-IR spectra were obtained on a Bruker 550 spectrometer.

### 3.3. Photocatalytic Activity

The photocatalytic activity of the catalysts was evaluated by the photocatalytic degradation of MO in aqueous solution. The photocatalysis experiments were performed in a batch reactor using a 500 W high-pressure Hg lamp as light source (Shanghai Bilang Co. Ltd), which was positioned 10 cm away from the batch reactor. A circulating water jacket was used to cool the batch reactor and the temperature was kept at around 25 °C. A 400 nm cut-off filter was used under the visible irradiation.

In a typical experiment, the reaction suspension consisting of MO aqueous solution (20 mg L<sup>-1</sup>, 150 mL) and catalyst (0.04 g) was stirred with a magnetic bar. Dioxygen was bubbled into the suspension. In all cases, the mixture was kept in the dark for 30 min to ensure that the adsorption-desorption equilibrium was reached before irradiation. After visible light or ultraviolet light irradiation, the sample was withdrawn from the suspension every 30 min during the irradiation for the determination of the absorbance change of MO. The catalyst was removed by centrifugation and remaining MO concentration in the solution was measured by light absorption of the clear solution at 464 nm.

## 4. Conclusions

In conclusion, *meso*-tetraphenyl metalloporphyrins (Fe, Co, Mn and Cu) adsorbed on TiO<sub>2</sub> (Degussa P25) photocatalysts were efficient for the degradation of MO aqueous solution under ultraviolet light irradiation. CuP-TiO<sub>2</sub> showed the most excellent activity for the photodegradation of MO no matter under visible or ultraviolet light irradiation. The DFT calculation results suggest that methyl orange ion is easier to be adsorbed by CuP-TiO<sub>2</sub> due to the more positive charge of Cu ion.

## Acknowledgements

The authors thank the National Natural Science Foundation of China (No. 20976203 and No. 21036009), higher-level talent project for Guangdong provincial universities and the Fundamental Research Funds for the Central Universities for providing financial support to this project.

## References and Notes

1. Zhao, J.; Li, B.; Onda, K.; Feng, M.; Petek, H. Solvated electrons on metal oxide surfaces. *Chem. Rev.* **2006**, *106*, 4402–4427.
2. Linsebigler, A.L.; Lu, G.Q.; Yates, J.T. Photocatalysis on TiO<sub>2</sub> surfaces: Principles, mechanisms, and selected results. *Chem. Rev.* **1995**, *95*, 735–758.
3. Hoffmann, M.R.; Martin, S.T.; Choi, W.; Bahnemann, D.W. Environmental applications of semiconductor photocatalysis. *Chem. Rev.* **1995**, *95*, 69–96.
4. Fox, M.A.; Dulay, M.T. Heterogeneous photocatalysis. *Chem. Rev.* **1993**, *93*, 341–347.
5. Ge, L. Novel visible-light-driven Pt/BiVO<sub>4</sub> photocatalyst for efficient degradation of methyl orange. *J. Mol. Catal. A* **2008**, *282*, 62–66.
6. Wang, X.J.; Liu, Y.F.; Hu, Z.H.; Chen, Y.J.; Liu, W.; Zhao, G.H. Degradation of methyl orange by composite photocatalysts nano-TiO<sub>2</sub> immobilized on activated carbons of different porosities. *J. Hazard. Mater.* **2009**, *169*, 1061–1067.

7. Li, X.Q.; Cheng, Y.; Kang, S.Z.; Mu, J. Preparation and enhanced visible light-driven catalytic activity of ZnO microrods sensitized by porphyrin heteroaggregate. *Appl. Surf. Sci.* **2010**, *256*, 6705–6709.
8. Zhang, W.J.; Wang, K.L.; Yu, Y.; He, H.B. TiO<sub>2</sub>/HZSM-5 nano-composite photocatalyst: HCl treatment of NaZSM-5 promotes photocatalytic degradation of methyl orange. *Chem. Eng. J.* **2010**, *163*, 62–67.
9. Rosas-Barrera, K.L.; Roper-Vega, J.L.; Pedraza-Avella, J.A.; Nino-Gomez, M.E.; Pedraza-Rosas, J.E.; Laverde-Catano, D.A. Photocatalytic degradation of methyl orange using Bi(2)MnO(7) (M= Al, Fe, Ga, In) semiconductor films on stainless steel. *Catal. Today* **2011**, *166*, 135–139.
10. Trejo-Tzab, R.; Alvarado-Gil, J.J.; Quintana, P. Photocatalytic activity of Degussa P25 TiO<sub>2</sub>/Au obtained using argon (Ar) and nitrogen (N<sub>2</sub>) plasma. *Top Catal.* **2011**, *54*, 250–256.
11. Yamanishi, K.; Miyazawa, M.; Yairi, T.; Sakai, S.; Nishina, N.; Kobori, Y.; Kondo, M.; Uchida, F. Conversion of cobalt(II) porphyrin into a helical cobalt(III) complex of acyclic pentapyrrole. *Angew. Chem. Int. Ed.* **2011**, *50*, 6583–6586.
12. Ren, Q.G.; Zhou, X.T.; Ji, H.B. Biomimetic models of nitric oxide synthase for the oxidation of oximes to carbonyl compounds catalyzed by water-soluble manganese porphyrins in aqueous solution. *J. Porphyr. Phthalocya.* **2011**, *15*, 211–216.
13. Che, C.M.; Lo, V.K.Y.; Zhou, C.Y.; Huang, J.S. Selective functionalisation of saturated C-H bonds with metalloporphyrin catalysts. *Chem. Soc. Rev.* **2011**, *40*, 1950–1975.
14. Mohammadi, K.; Hasaninejad, A.; Niad, M.; Najmi, M. Application of metalloporphyrins as new catalysts for the efficient, mild and regioselective synthesis of quinoxaline derivatives. *J. Porphyr. Phthalocya.* **2010**, *14*, 1052–1058.
15. Ji, H.B.; Zhou, X.T. Biomimetic homogeneous oxidation catalyzed by metalloporphyrins with green oxidants. In *Biomimetics, Learning from Nature*; In-Tech Publishing: Vienna, Austria, 2010.
16. Meunier, B.; de Visser, S.P.; Shaik, S. Mechanism of oxidation reactions catalyzed by cytochrome P450 enzymes. *Chem. Rev.* **2004**, *104*, 3947–3980.
17. Cho, Y.M.; Choi, W.Y.; Lee, C.H.; Hyeon, T.; Lee, H.I. Visible light-induced degradation of carbon tetrachloride on dye-sensitized TiO<sub>2</sub>. *Environ. Sci. Technol.* **2001**, *35*, 966–970.
18. Wang, C.; Li, J.; Mele, G.; Yang, G.M.; Zhang, F.X.; Palmisano, L.; Vasapollo, G. Efficient degradation of 4-nitrophenol by using functionalized porphyrin-TiO<sub>2</sub> photocatalysts under visible irradiation. *Appl. Catal. B* **2007**, *76*, 218–226.
19. Granados-Oliveros, G.; Paez-Mozo, E.A.; Ortega, F.M.; Ferronato, C.; Chovelon, J.M. Degradation of atrazine using metalloporphyrins supported on TiO<sub>2</sub> under visible light irradiation. *Appl. Catal. B* **2009**, *89*, 448–454.
20. Gokakakar, S.D.; Salker, A.V. Solar assisted photocatalytic degradation of methyl orange over synthesized copper, silver and tin metalloporphyrins. *Indian J. Chem. Techn.* **2009**, *16*, 492–498.
21. Ohtani, B.; Prieto-Mahaney, O.O.; Li, D.; Abe, R. What is Degussa (Evonik) P25? Crystalline composition analysis, reconstruction from isolated pure particles and photocatalytic activity test. *J. Photoch. Photobio. A* **2010**, *216*, 179–182.

22. Mele, G.; Del Sole, R.; Vasapollo, G.; Garcia-Lopez, E.; Palmisano, L.; Schiavello, M. Photocatalytic degradation of 4-nitrophenol in aqueous suspension by using polycrystalline TiO<sub>2</sub> impregnated with functionalized Cu(II)-porphyrin or Cu(II)-phthalocyanine. *J. Catal.* **2003**, *217*, 334–342.
23. Duan, M.Y.; Li, J.; Mele, G.; Wang, C.; Lu, X.F.; Vasapollo, G.; Zhang, F.X. Photocatalytic activity of novel tin porphyrin/TiO<sub>2</sub> based composites. *J. Phys. Chem. C* **2010**, *114*, 7857–7862.
24. Hilal, H.S.; Majjad, L.Z.; Zaatari, N.; El-Hamouz, A. Dye-effect in TiO<sub>2</sub> catalyzed contaminant photo-degradation: Sensitization vs. charge-transfer formalism. *Solid State Sci.* **2007**, *9*, 9–15.
25. Wang, C.; Yang, G.M.; Li, J.; Mele, G.; Slota, R.; Broda, M.A.; Duan, M.Y.; Vasapollo, G.; Zhang, X.; Zhang, F.X. Novel meso-substituted porphyrins: Synthesis, characterization and photocatalytic activity of their TiO<sub>2</sub>-based composites. *Dyes Pigments* **2009**, *80*, 321–328.
26. Wang, C.; Li, J.; Mele, G.; Duan, M.Y.; Lu, X.F.; Palmisano, L.; Vasapollo, G.; Zhang, F.X. The photocatalytic activity of novel, substituted porphyrin/TiO<sub>2</sub>-based composites. *Dyes Pigments* **2010**, *84*, 183–189.
27. Frisch, M.J. Gaussian W03, Revision D. 01; Gaussian, Inc.: Wallingford, CT, USA, 2004.
28. Zhou, X.T.; Ji, H.B.; Yuan, Q.L. Baeyer-Villiger oxidation of ketones catalyzed by iron(III) meso-tetraphenylporphyrin chloride in the presence of molecular oxygen. *J. Porphyr. Phthalocya.* **2008**, *12*, 94–100.

*Sample Availability:* Samples of the compounds are available from the authors (or from MDPI).

© 2012 by the authors; licensee MDPI, Basel, Switzerland. This article is an open access article distributed under the terms and conditions of the Creative Commons Attribution license (<http://creativecommons.org/licenses/by/3.0/>).